Active Galactic Nuclei

Sergio A. Cellone[1,2]

[1] Facultad de Ciencias Astronómicas y Geofísicas
Universidad Nacional de La Plata, Argentina

[2] Instituto de Astrofísica La Plata
CONICET – UNLP

LAPIS 2008

FCAG, UNLP — AAA

Contents

Active Galactic Nuclei

Wild beasts in the astronomical zoo . . .

(. . . long before GARRA)

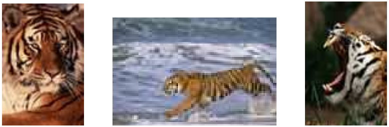

- Seyfert galaxies,
- radio galaxies,
- and quasars.

Wild beasts in the astronomical zoo . . .

(. . . long before GARRA)



- Seyfert galaxies,
- radio galaxies,
- and quasars.

Wild beasts in the astronomical zoo . . .

(. . . long before GARRA)



- Seyfert galaxies,
- radio galaxies,
- and quasars.

Wild beasts in the astronomical zoo . . .

(. . . long before GARRA)

  

- Seyfert galaxies,
- radio galaxies,
- and quasars.

Seyfert galaxies

Fath 1909: strong emission lines
in the optical spectrum
of the "spiral nebula" NGC 1068

Slipher 1917: emissions in NGC 1068
were not monochromatic
(i.e., broad)

Hubble 1926: a few spiral galaxies with stellar nuclei
had optical spectra similar to planetary nebulæ

Seyfert galaxies

Fath 1909: strong emission lines
in the optical spectrum
of the “spiral nebula” NGC 1068

Slipher 1917: emissions in NGC 1068
were not monochromatic
(i.e., broad)

Hubble 1926: a few spiral galaxies with stellar nuclei
had optical spectra similar to planetary nebulæ

Seyfert galaxies

Fath 1909: strong emission lines
in the optical spectrum
of the “spiral nebula” NGC 1068

Slipher 1917: emissions in NGC 1068
were not monochromatic
(i.e., broad)

Hubble 1926: a few spiral galaxies with stellar nuclei
had optical spectra similar to planetary nebulæ

Seyfert galaxies

Carl Seyfert (1943)

started the systematic study of
spiral galaxies with stellar-like nuclei.
They showed composite optical spectra:

G-type starlight ($\equiv$ normal galaxy)
$+$
strong, high excitation emission lines.

Seyfert galaxies
Images

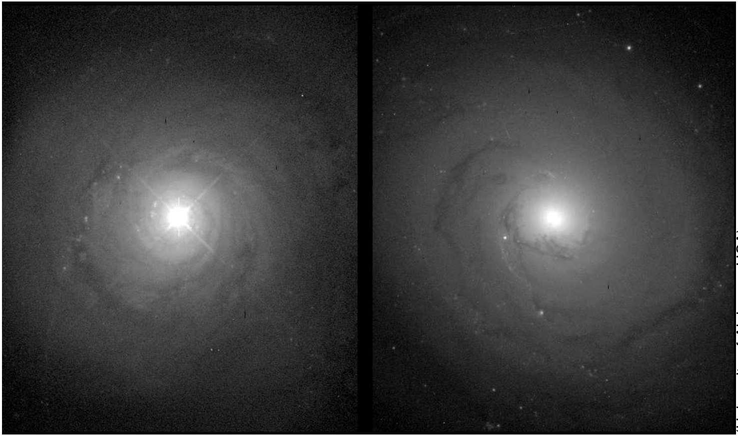
(University of Alabama, USA)

NGC 5548 (Seyfert galaxy) NGC 3277 (normal Sbc)

Seyfert galaxies

Spectra

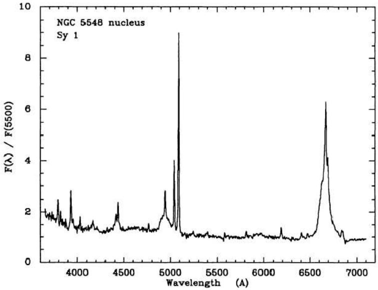

NGC 5548 (Seyfert galaxy)

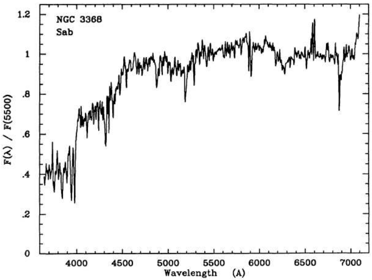

NGC 3368 (normal Sbc)

(Kennicutt 1992)

Radio galaxies

- Up to 1609 (G. Galilei): milennia of naked-eye Astronomy
- 1609 - 1935 (K. Jansky): 3 centuries of optical telescopes

Optical identification of radio sources was (is) needed.

First (discrete) radio-sources identified (Bolton et al. 1949)

Tau A	≡	Crab Nebula	(SNR)
Vir A	≡	M87	(radio galaxy)
Cen A	≡	NGC 5128	(radio galaxy)

Radio galaxies

- Up to 1609 (G. Galilei): milennia of naked-eye Astronomy
- 1609 - 1935 (K. Jansky): 3 centuries of optical telescopes

Optical identification of radio sources was (is) needed.

First (discrete) radio-sources identified (Bolton et al. 1949)

Tau A	$\equiv$	Crab Nebula	(SNR)
Vir A	$\equiv$	M87	(radio galaxy)
Cen A	$\equiv$	NGC 5128	(radio galaxy)

Radio galaxies

Note

Radio continuum:
$\nu = 60 - 80 - 100$ Mhz ($\equiv \lambda = 5.0 - 3.7 - 2.0\,$m, respec.)
Non-thermal spectrum (synchrotron radiation)

The HI 21 cm ($\equiv$ 1.4 Ghz) line would not be detected until 1951

Radio galaxies

Note

Radio continuum:
$\nu = 60 - 80 - 100$ Mhz ($\equiv \lambda = 5.0 - 3.7 - 2.0$ m, respec.)
Non-thermal spectrum (synchrotron radiation)

The HI 21 cm ($\equiv$ 1.4 Ghz) line would not be detected until 1951

Radio galaxies

Jennison & Das Gupta (1953):
radio source Cyg A $\longrightarrow$ two-component radio morphology

Baade & Minkowski (1954):
optical object $\sim$ “two colliding galaxies”
$z = 0.056 \;\Rightarrow\; L_{\rm rad} \approx 6 \times 10^{43}\,\mathrm{erg\,s^{-1}}$ ($H_0 = 70\;\mathrm{km\,s^{-1}Mpc^{-1}}$).

Radio Image of Cygnus-A (FR-II)

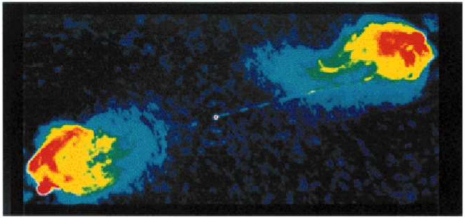

z=0.056 (d≈300 Mpc) 5 GHz image ; Ø 200 kpc

Radio galaxies

Jennison & Das Gupta (1953):
radio source Cyg A $\longrightarrow$ two-component radio morphology

Baade & Minkowski (1954):
optical object $\sim$ "two colliding galaxies"
$z = 0.056 \;\Rightarrow\; L_{\rm rad} \approx 6 \times 10^{43}\,{\rm erg\,s^{-1}}$ ($H_0 = 70\;{\rm km\,s^{-1}Mpc^{-1}}$).

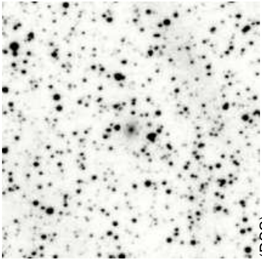
(DSS)

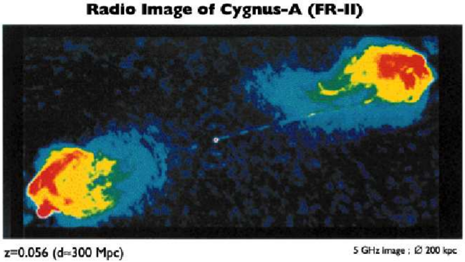

Quasars

Edge et al. (1959): 3rd Cambridge survey of radio sources

A. Sandage (1960): radio-source 3C 48 $\equiv$ 16 mag, variable star-like object

Matthews & Sandage (1963): optical spectrum with broad unknown emission lines

Quasars

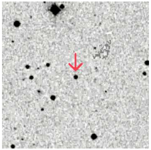

Edge et al. (1959): 3^{rd} Cambridge survey of radio sources

A. Sandage (1960): radio-source 3C 48 $\equiv$ 16 mag, variable star-like object

Matthews & Sandage (1963): optical spectrum with broad unknown emission lines

Quasi-stellar radio-sources
(QSRS or QSS) $\longrightarrow$ quasar

Quasars

Edge et al. (1959): 3^{rd} Cambridge survey of radio sources

A. Sandage (1960): radio-source 3C 48 $\equiv$ 16 mag, variable star-like object

Matthews & Sandage (1963): optical spectrum with broad unknown emission lines

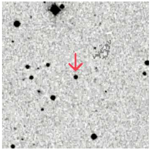

Quasi-stellar radio-sources
(QSRS or QSS) $\longrightarrow$ quasar

Quasars

Edge et al. (1959): 3^{rd} Cambridge survey of radio sources

A. Sandage (1960): radio-source 3C 48 $\equiv$ 16 mag, variable star-like object

Matthews & Sandage (1963): optical spectrum with broad unknown emission lines

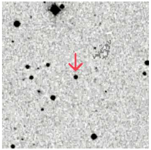

Quasi-stellar radio-sources
(QSRS or QSS) $\longrightarrow$ quasar

Quasars

3C 273

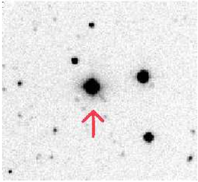

Maarten Schmidt (1963): optical spectrum

Quasars

3C 273

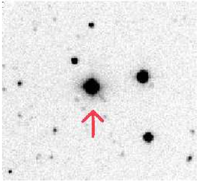

Maarten Schmidt (1963): optical spectrum

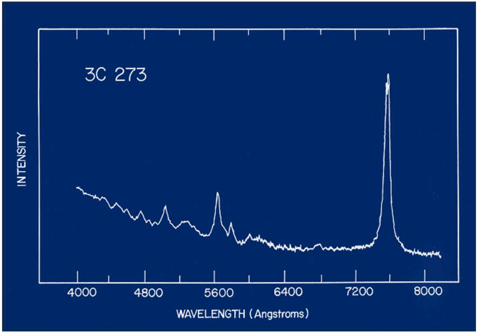

Quasars

3C 273

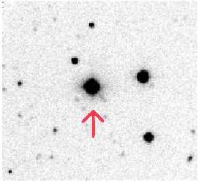

Maarten Schmidt (1963): optical spectrum

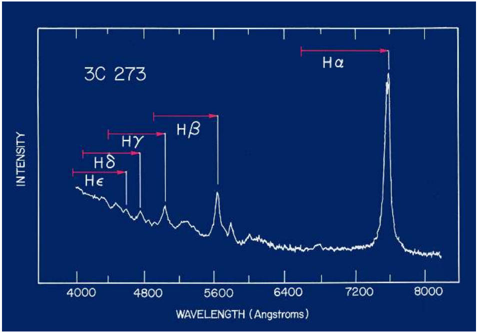

$z = 0.158$

Quasars

Quasars have high redshifts

Doppler redshifts: Nearby objects moving at high speeds

- no proper motions
- no blueshifts

Gravitational redshifts: supermassive object (GR)

- extremely high electron densities (no forbidden lines should be observed)

Cosmological redshifts: $d \simeq c\,z\,H_0^{-1}$ (for $z \ll 1$)

- $L_{\rm opt} \geq 10 - 30$ times bright E galaxy
- size $\ll$ normal galaxy

Quasars

Quasars have high redshifts

Doppler redshifts: Nearby objects moving at high speeds

- no proper motions
- no blueshifts

Gravitational redshifts: supermassive object (GR)

- extremely high electron densities (no forbidden lines should be observed)

Cosmological redshifts: $d \simeq c\,z\,H_0^{-1}$ (for $z \ll 1$)

- $L_{\rm opt} \geq 10 - 30$ times bright E galaxy
- size $\ll$ normal galaxy

Quasars

Quasars have high redshifts

Doppler redshifts: Nearby objects moving at high speeds

- no proper motions
- no blueshifts

Gravitational redshifts: supermassive object (GR)

- extremely high electron densities (no forbidden lines should be observed)

Cosmological redshifts: $d \simeq c\,z\,H_0^{-1}$ (for $z \ll 1$)

- $L_{opt} \geq 10 - 30$ times bright E galaxy
- size $\ll$ normal galaxy

Quasars

Quasars have high redshifts

Doppler redshifts: Nearby objects moving at high speeds

- no proper motions
- no blueshifts

Gravitational redshifts: supermassive object (GR)

- extremely high electron densities
  (no forbidden lines should be observed)

Cosmological redshifts: $d \simeq c\,z\,H_0^{-1}$ (for $z \ll 1$)

- $L_{\rm opt} \geq 10 - 30$ times bright E galaxy
- size $\ll$ normal galaxy

Quasars

Quasars have high redshifts

Doppler redshifts: Nearby objects moving at high speeds

- no proper motions
- no blueshifts

Gravitational redshifts: supermassive object (GR)

- extremely high electron densities
  (no forbidden lines should be observed)

Cosmological redshifts: $d \simeq c\,z\,H_0^{-1}$ (for $z \ll 1$)

- $L_{\rm opt} \geq 10 - 30$ times bright E galaxy
- size $\ll$ normal galaxy

Quasars

Quasars have high redshifts

Doppler redshifts: Nearby objects moving at high speeds

- no proper motions
- no blueshifts

Gravitational redshifts: supermassive object (GR)

- extremely high electron densities (no forbidden lines should be observed)

Cosmological redshifts: $d \simeq c\,z\,H_0^{-1}$ (for $z \ll 1$)

- $L_{\rm opt} \geq 10 - 30$ times bright E galaxy
- size $\ll$ normal galaxy

Quasars

Quasars have high redshifts

Doppler redshifts: Nearby objects moving at high speeds

- no proper motions
- no blueshifts

Gravitational redshifts: supermassive object (GR)

- extremely high electron densities (no forbidden lines should be observed)

Cosmological redshifts: $d \simeq c\, z\, H_0^{-1}$ (for $z \ll 1$)

- $L_{\rm opt} \geq 10 - 30$ times bright E galaxy
- size $\ll$ normal galaxy

Quasars

Quasars have high redshifts

Doppler redshifts: Nearby objects moving at high speeds

- no proper motions
- no blueshifts

Gravitational redshifts: supermassive object (GR)

- extremely high electron densities (no forbidden lines should be observed)

Cosmological redshifts: $d \simeq c\,z\,H_0^{-1}$ (for $z \ll 1$)

- $L_{\rm opt} \geq 10-30$ times bright E galaxy
- size $\ll$ normal galaxy

Quasars

Sandage (1965): quasars have U excess

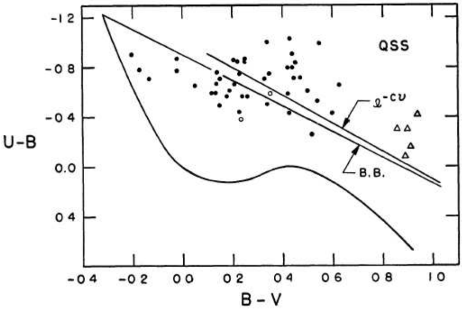

Large population of radio-quiet quasars

quasi-stellar objects → *QSO*

Origins of the SMBH model

Salpeter (1964); Zel'dovich & Novikov (1964): Energy source in quasars and radio galaxies is accretion onto a super-massive black hole (SMBH)

Lynden-Bell (1969):

energy in radio-galaxies (lobes) $\longrightarrow$ $E_{\rm RG} \sim 10^{61}$ erg.
Its associated mass is:

$$\mathcal{M}_E = E_{\rm RG}\, c^{-2} \simeq 6 \times 10^6\, \mathcal{M}_\odot,$$

if result of nuclear burning, requires an original mass

$$\mathcal{M} \geq \frac{\mathcal{M}_E}{0.007} \simeq 10^9\, \mathcal{M}_\odot.$$

Origins of the SMBH model

Salpeter (1964); Zel'dovich & Novikov (1964): Energy source in quasars and radio galaxies is accretion onto a super-massive black hole (SMBH)

Lynden-Bell (1969):

energy in radio-galaxies (lobes) $\rightarrow$ $E_{\rm RG} \sim 10^{61}$ erg.
Its associated mass is:

$$\mathcal{M}_E = E_{\rm RG}\, c^{-2} \simeq 6 \times 10^6\, \mathcal{M}_\odot,$$

if result of nuclear burning, requires an original mass

$$\mathcal{M} \geq \frac{\mathcal{M}_E}{0.007} \simeq 10^9 \mathcal{M}_\odot.$$

Origins of the SMBH model

Salpeter (1964); Zel'dovich & Novikov (1964): Energy source in quasars and radio galaxies is accretion onto a super-massive black hole (SMBH)

Lynden-Bell (1969):

energy in radio-galaxies (lobes) $\rightarrow$ $E_{\mathrm{RG}} \sim 10^{61}$ erg.
Its associated mass is:

$$\mathcal{M}_E = E_{\mathrm{RG}}\, c^{-2} \simeq 6 \times 10^6\, \mathcal{M}_\odot,$$

if result of nuclear burning, requires an original mass

$$\mathcal{M} \geq \frac{\mathcal{M}_E}{0.007} \simeq 10^9 \mathcal{M}_\odot.$$

Origins of the SMBH model

Lynden-Bell (1969):

Variability $\Rightarrow$ $R \leq 10$ light-hs $= 10^{15}$ cm.

Binding energy

$$\frac{G\mathcal{M}^2}{R} \simeq 2.7 \times 10^{62}\ \text{erg}.$$

Thus, with the aim to produce a model based on nuclear fuel, we have ended up with a model which has produced more than enough energy by gravitational contraction, while nuclear fuel has ended as an irrelevance.

Origins of the SMBH model

Lynden-Bell (1969):

Variability $\Rightarrow$ $R \leq 10$ light-hs $= 10^{15}$ cm.

Binding energy

$$\frac{G\mathcal{M}^2}{R} \simeq 2.7 \times 10^{62}\,\text{erg}.$$

Thus, with the aim to produce a model based on nuclear fuel, we have ended up with a model which has produced more than enough energy by gravitational contraction, while nuclear fuel has ended as an irrelevance.

Origins of the SMBH model

Lynden-Bell (1969):

Variability $\Rightarrow$ $R \leq 10$ light-hs $= 10^{15}$ cm.

Binding energy

$$\frac{G\mathcal{M}^2}{R} \simeq 2.7 \times 10^{62}\,\mathrm{erg}.$$

Thus, with the aim to produce a model based on nuclear fuel, we have ended up with a model which has produced more than enough energy by gravitational contraction, while nuclear fuel has ended as an irrelevance.

Sy + RG + QSO = AGN

Seyfert nuclei & radio galaxies:
scaled-down versions of QSO

Do quasars reside at the centres of galaxies?

Sy + RG + QSO = AGN

Seyfert nuclei & radio galaxies:
scaled-down versions of QSO

Do quasars reside at the centres of galaxies?

Sy + RG + QSO = AGN

Quasars lie at the centres of galaxies

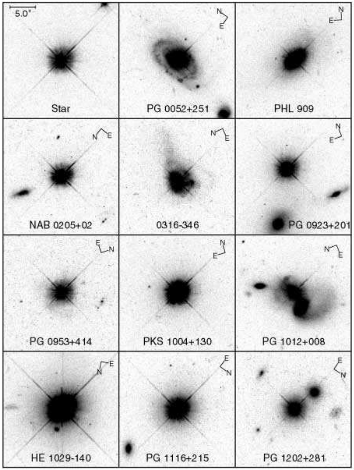

(Bahcall et al. 1997)

Sy + RG + QSO = AGN

Active Galactic Nuclei (AGN)

- Seyfert galaxies,
- radio galaxies,
- quasars (and blazars)

Active Galactic Nuclei

What do we mean by *high-excitation*?

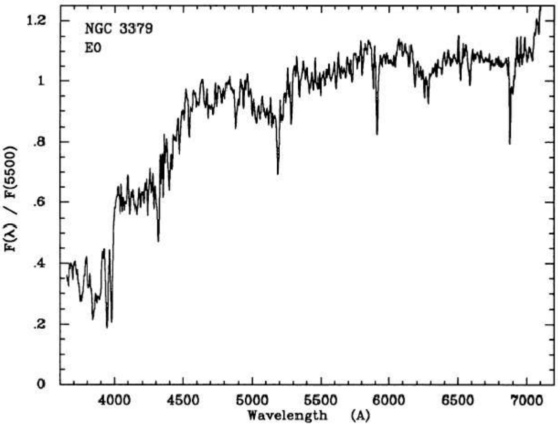

(Kennicutt 1992)

normal E galaxy

What do we mean by *high-excitation*?

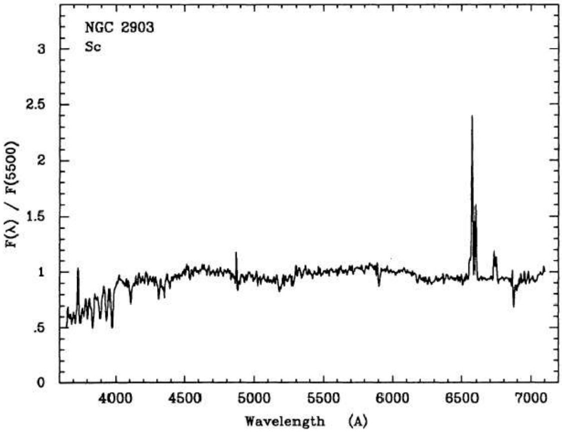

(Kennicutt 1992)

normal Sc galaxy

What do we mean by *high-excitation*?

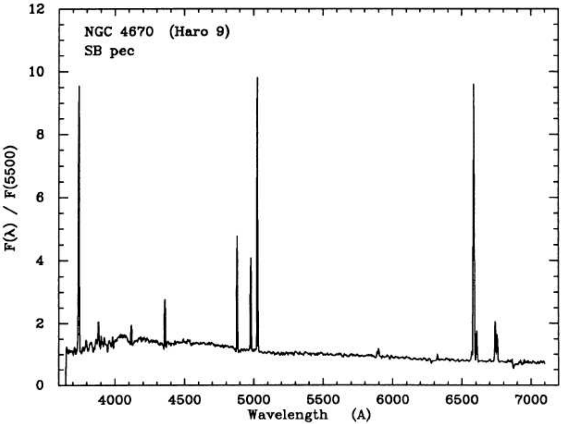

(Kennicutt 1992)

magellanic spiral

What do we mean by *high-excitation*?

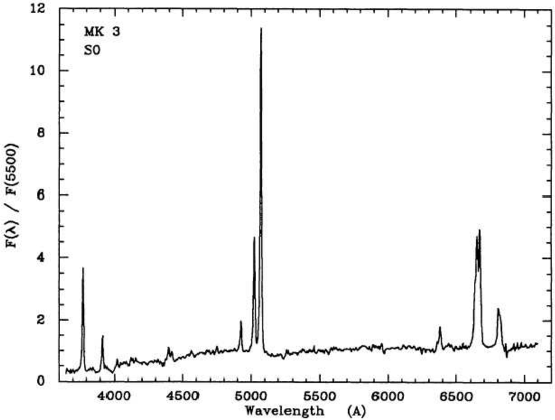

(Kennicutt 1992)

Seyfert (2)

What do we mean by *high-excitation*?

Diagnostic diagrams

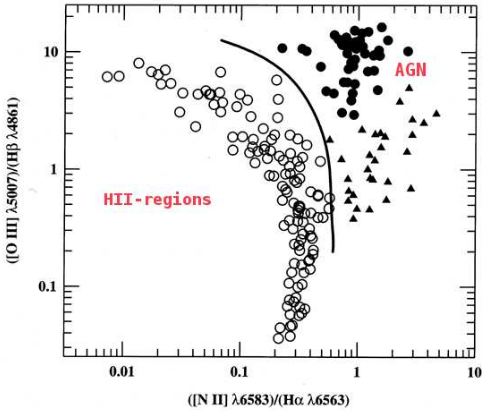

Diagnostic diagram (Baldwin, Phillips, & Terlevich 1981)

What do we mean by *high-excitation*?

Diagnostic diagrams

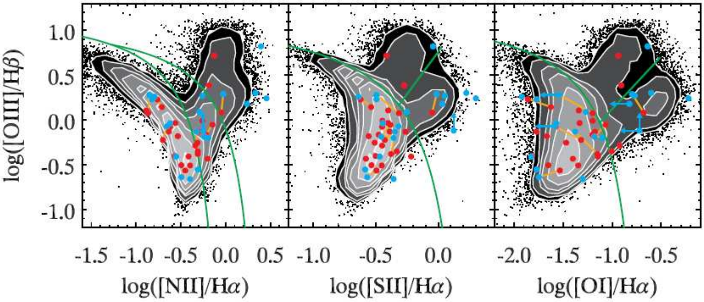

Sloan Digital Sky Survey (SDSS)

Seyfert types 1 and 2

Seyfert 1

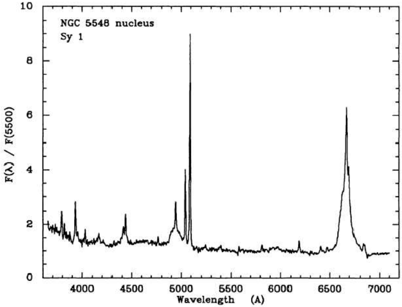

Seyfert 2

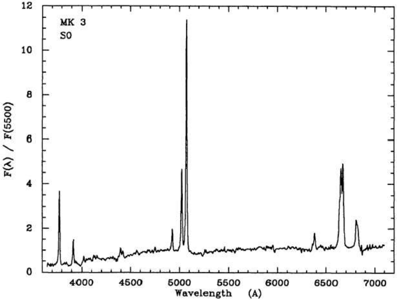

broad lines: only permitted

broad lines: none

narrow lines: permitted and prohibited

Quasars

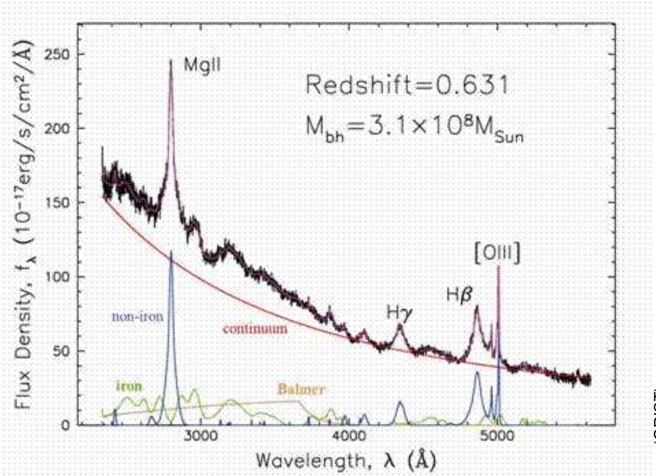

(GRIST)

BL Lac objects

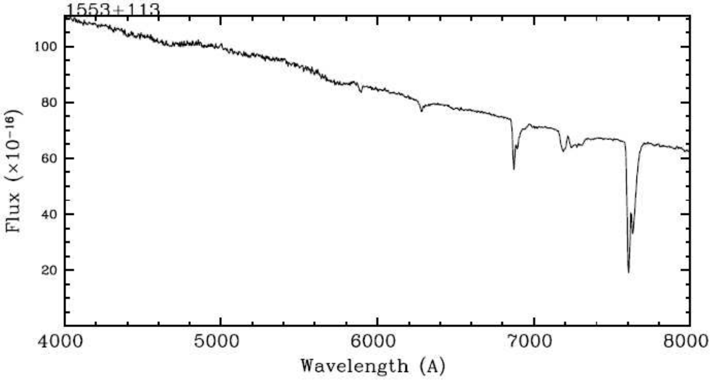

(Boris Sbarufatti)

BL Lac objects

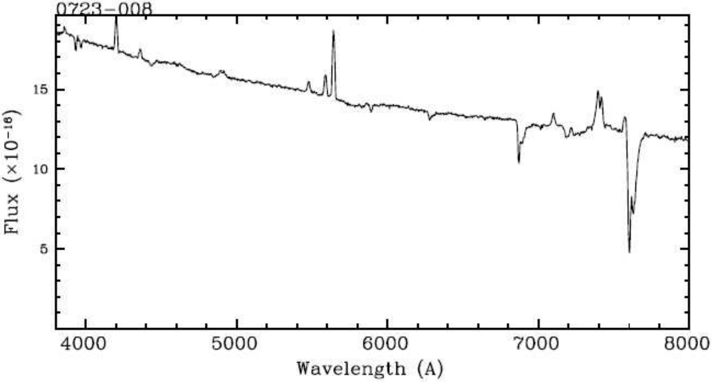

(Boris Sbarufatti)

Continuum spectral energy distribution

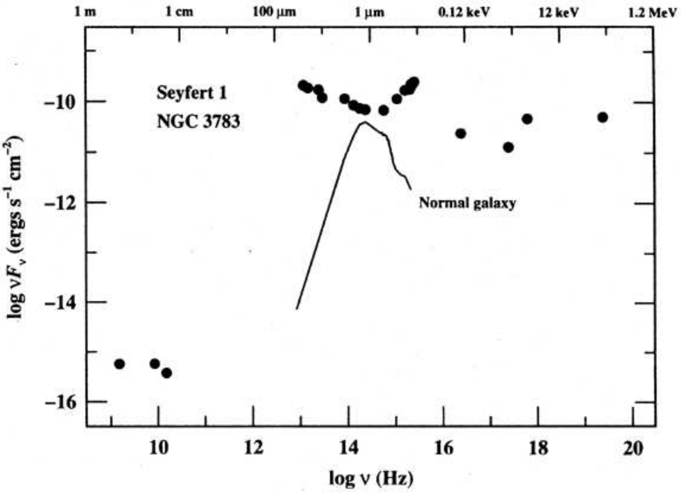

Continuum spectral energy distribution

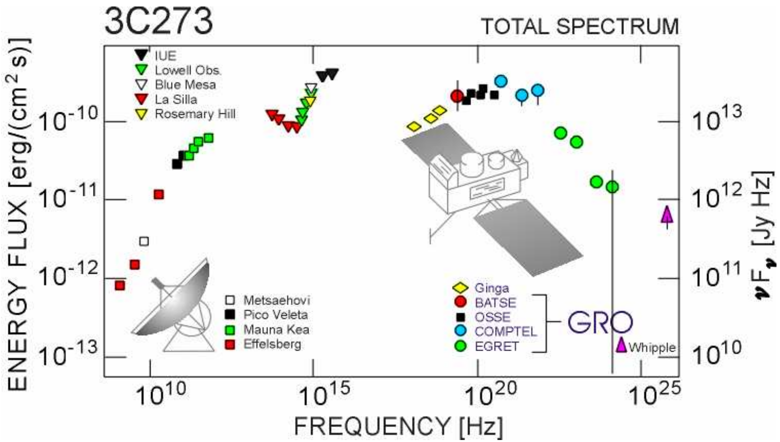

Radio emission

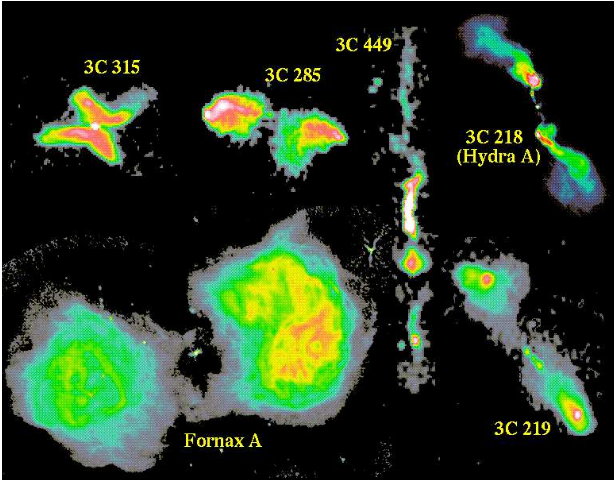

("Images from the Invisible Universe", NRAO)

21 cm (1.4 GHz) VLA – 11 cm (2.7 GHz) MRAO

Radio emission

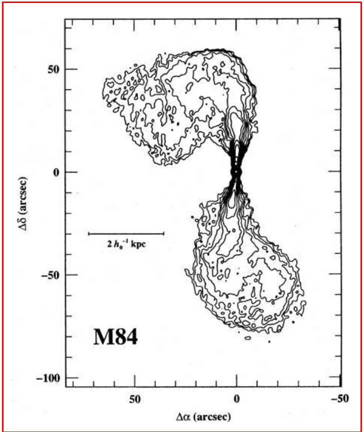

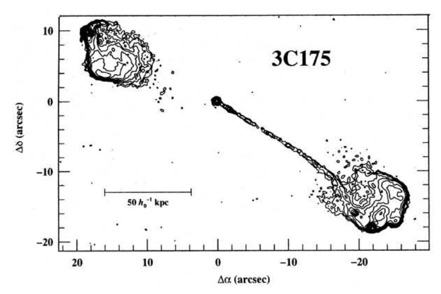

Fanaroff-Riley class II – (FR II)

Fanaroff-Riley class I – (FR I)

Jets

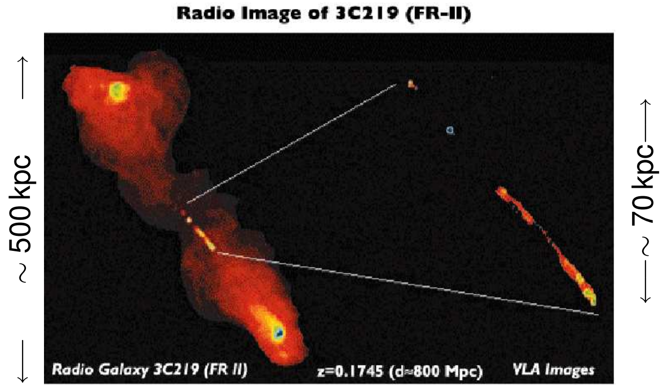

Radio lobes: *steep* spectrum
Jets: *flat* spectrum

Jets

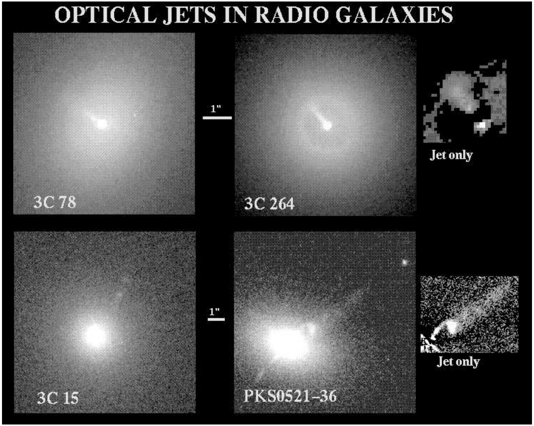

(HST images by S. Baum & A. Martel)

Jets

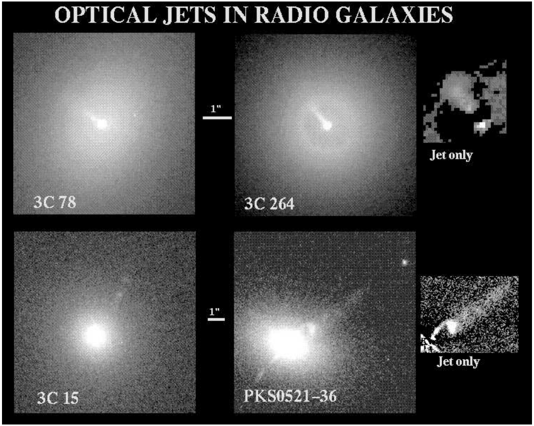

(HST images by S. Baum & A. Martel)

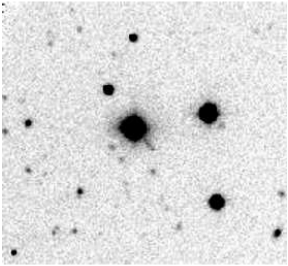

3C 273

Jets

Apparent superluminal motions

$\longleftarrow$ 5 mas $\equiv$ 30 pc $\longrightarrow$

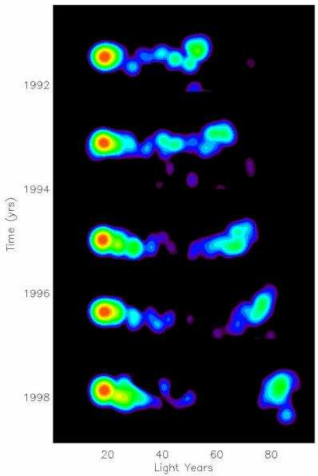

(Image courtesy of NRAO/AUI)

Radio jet of the blazar 3C 279
$\sim$ 25 light-years in $\sim$ 7 yr

$$\therefore \quad v_{\text{app}} \simeq 3.5\, c$$

Jets
Apparent superluminal motions

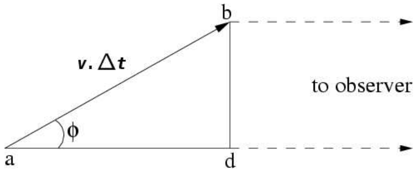

$$\beta_{\rm app} = \frac{\beta \sin\phi}{1-\beta\cos\phi} \qquad (\beta = \frac{v}{c})$$

$$\beta \lesssim 1 \text{ and } \phi \gtrsim 0 \quad \Rightarrow \quad \beta_{\rm app} > 1$$

Long-term variability

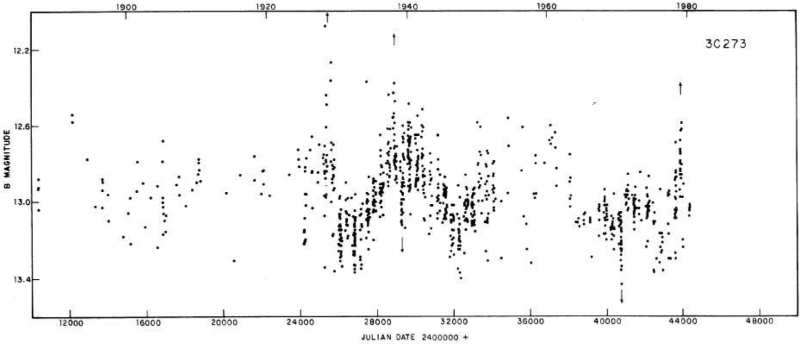

quasar 3C 273

historical light-curve (Angione & Smith 1985): $\Delta m \simeq 1$ mag

Long-term variability

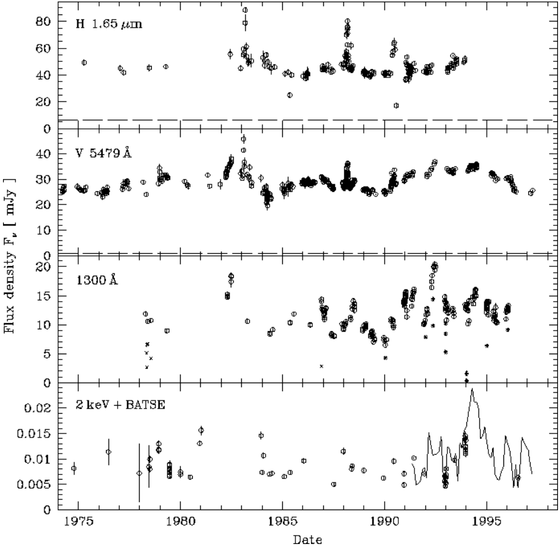

quasar 3C 273

multi-ν light-curve (Türler et al. 1999):

Long-term variability

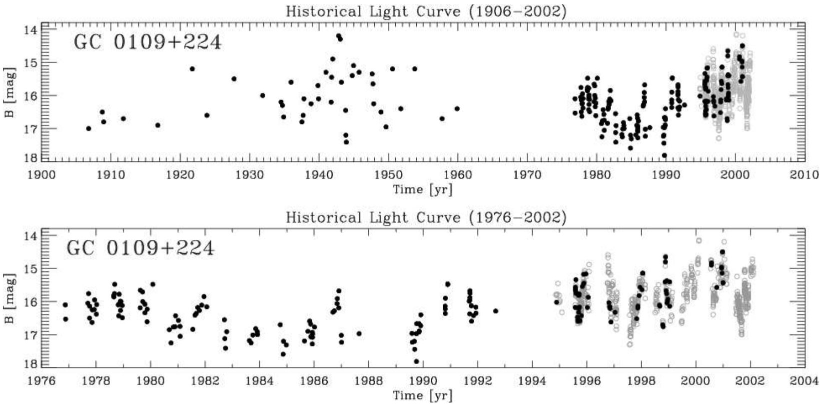

blazar GC 0109+224

historical light-curve (Ciprini et al. 2003): $\Delta m \simeq 4\,\mathrm{mag}$

Long-term variability

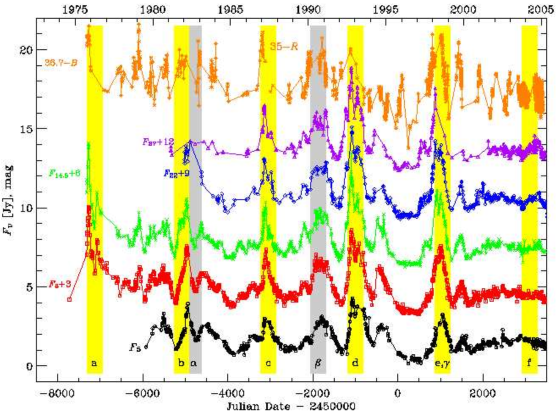

blazar
AO 0235+164
optical – radio light-curve
(Raiteri et al. 2006)
$\Delta m \gtrsim 7\,\mathrm{mag}$

Microvariability

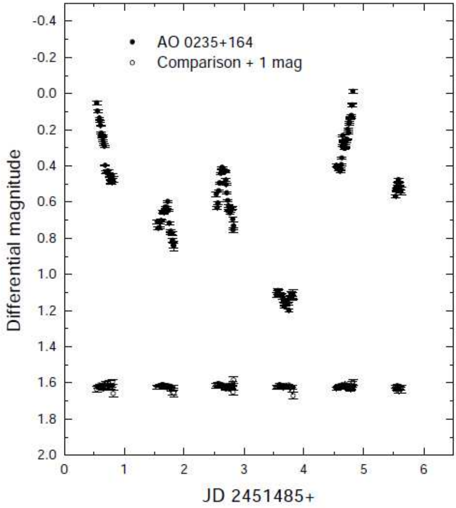

blazar AO 0235+164

optical microvariability:

1.2 mag in $\gtrsim$ 24 hs

(Romero et al. 2000)

Polarization microvariability

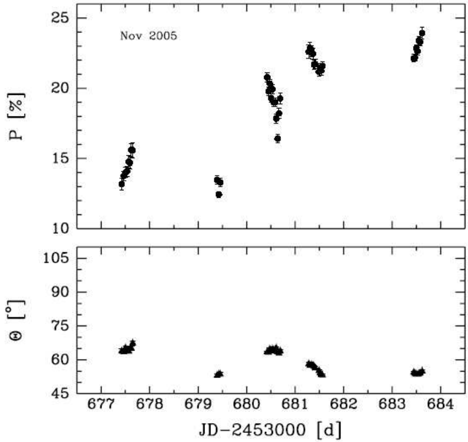

blazar AO 0235+164

high and variable optical polarization:
$\Delta P \simeq 10\,\%$ in $\gtrsim 48$ hs
(Cellone et al. 2007)

Polarization microvariability

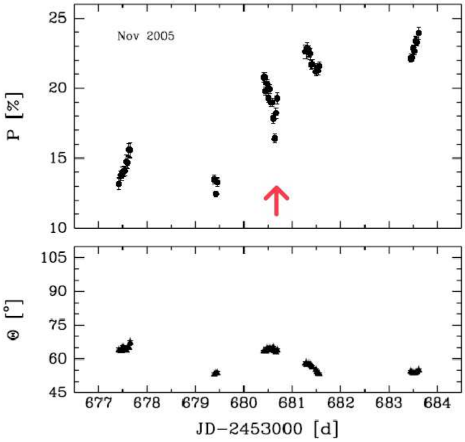

blazar AO 0235+164

high and variable optical polarization:
$\Delta P \simeq 10\,\%$ in $\gtrsim 48\,$hs
(Cellone et al. 2007)

Polarization microvariability

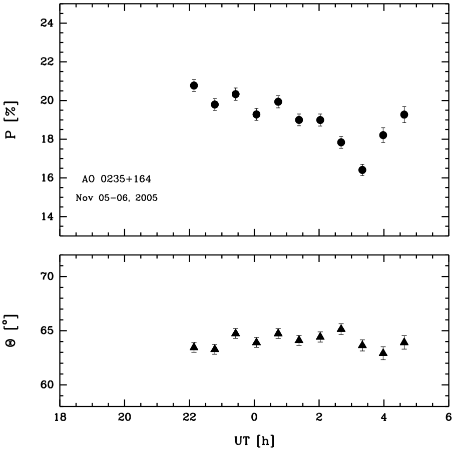

blazar AO 0235+164

high and variable optical polarization:
$\Delta P \simeq 5\,\%$ in ~ 5 hs
(Cellone et al. 2007)

Active Galactic Nuclei

Basic properties of AGN

AGN have:

High luminosity: $\sim 10^{42} \rightarrow 10^{48}\,\mathrm{erg\,s^{-1}}$
i.e., $\sim 10^{-2} \rightarrow 10^{4}\ L_{\star}$

Small size: central engine $\lesssim 10^{0}$ pc

- unresolved in nearby AGN
- variability time-scale $\sim$ few years

Long life: $\sim 10^{9}$ yr

- luminosity function with z
- density AGN vs. density bright galaxies

Basic properties of AGN

AGN have:

High luminosity: $\sim 10^{42} \rightarrow 10^{48}\,\mathrm{erg\,s^{-1}}$
i.e., $\sim 10^{-2} \rightarrow 10^{4}\ L_{\star}$

Small size: central engine $\lesssim 10^{0}\,\mathrm{pc}$

- unresolved in nearby AGN
- variability time-scale $\sim$ few years

Long life: $\sim 10^{9}$ yr

- luminosity function with z
- density AGN vs. density bright galaxies

Basic properties of AGN

AGN have:

High luminosity: $\sim 10^{42} \rightarrow 10^{48}\,\mathrm{erg\,s^{-1}}$
i.e., $\sim 10^{-2} \rightarrow 10^{4}\ L_{\star}$

Small size: central engine $\lesssim 10^{0}\,\mathrm{pc}$

- unresolved in nearby AGN
- variability time-scale $\sim$ few years

Long life: $\sim 10^{9}$ yr

- luminosity function with z
- density AGN vs. density bright galaxies

Energy production

Most efficient way to release energy:

accretion into a relativistically deep gravitational potential

$$\epsilon \sim 0.1$$

Eddington luminosity

Acceleration due to radiation pressure:

$$a_{\rm rad} = \frac{\sigma_{\rm T}}{\mu_{\rm p}} \frac{L}{4\pi c\, r^2}$$

$$\Rightarrow \quad \frac{a_{\rm rad}}{g} = \frac{\sigma_{\rm T}\, L}{4\pi c\, \mu_{\rm p}\, G\, \mathcal{M}_\bullet} = \frac{L}{L_{\rm E}}$$

where

$$L_{\rm E} = \frac{4\pi c\, G\, \mathcal{M}_\bullet\, \mu_{\rm p}}{\sigma_{\rm T}} = 1.51 \times 10^{38} \frac{\mathcal{M}_\bullet}{\mathcal{M}_\odot}\, {\rm erg\, s^{-1}}$$

$$\therefore \quad L = 10^{47}\, {\rm erg\, s^{-1}} \Rightarrow \mathcal{M}_\bullet = 10^9\, \mathcal{M}_\odot$$

Eddington luminosity

Acceleration due to radiation pressure:

$$a_{\mathrm{rad}} = \frac{\sigma_{\mathrm{T}}}{\mu_{\mathrm{p}}} \frac{L}{4\pi c\, r^2}$$

$$\Rightarrow \quad \frac{a_{\mathrm{rad}}}{g} = \frac{\sigma_{\mathrm{T}}\, L}{4\pi c\, \mu_{\mathrm{p}}\, G \mathcal{M}_\bullet} = \frac{L}{L_{\mathrm{E}}}$$

where

$$L_{\mathrm{E}} = \frac{4\pi c\, G \mathcal{M}_\bullet\, \mu_{\mathrm{p}}}{\sigma_{\mathrm{T}}} = 1.51 \times 10^{38} \frac{\mathcal{M}_\bullet}{\mathcal{M}_\odot}\, \mathrm{erg\, s}^{-1}$$

$$\therefore \quad L = 10^{47}\, \mathrm{erg\, s}^{-1} \Rightarrow \mathcal{M}_\bullet = 10^{9}\, \mathcal{M}_\odot$$

Eddington luminosity

Acceleration due to radiation pressure:

$$a_{\rm rad} = \frac{\sigma_{\rm T}}{\mu_{\rm p}} \frac{L}{4\pi c\, r^2}$$

$$\Rightarrow \qquad \frac{a_{\rm rad}}{g} = \frac{\sigma_{\rm T}\, L}{4\pi c\, \mu_{\rm p}\, G\, \mathcal{M}_\bullet} = \frac{L}{L_{\rm E}}$$

where

$$L_{\rm E} = \frac{4\pi c\, G\, \mathcal{M}_\bullet\, \mu_{\rm p}}{\sigma_{\rm T}} = 1.51 \times 10^{38} \frac{\mathcal{M}_\bullet}{\mathcal{M}_\odot}\, {\rm erg\, s^{-1}}$$

$$\therefore \qquad L = 10^{47}\, {\rm erg\, s^{-1}} \Rightarrow \mathcal{M}_\bullet = 10^9\, \mathcal{M}_\odot$$

Nature of the engine

Need for a large mass

- energy output
- Eddington luminosity
- broad emission lines
- relativistic outflows (jets)

Nature of the massive object(s)

single super-massive black hole (SMBH)

- stability
- coherent variability
- well collimated jets

Phenomenology

The model should also be able to explain:

- nature of continuum emission
- nature of line emission
- broad lines vs. narrow lines
- radio loud vs. radio quiet
- jets & radio lobes
- blazar phenomenology

Phenomenology

The model should also be able to explain:

- nature of continuum emission
- nature of line emission
- broad lines vs. narrow lines
- radio loud vs. radio quiet
- jets & radio lobes
- blazar phenomenology

Phenomenology

The model should also be able to explain:

- nature of continuum emission
- nature of line emission
- broad lines vs. narrow lines
- radio loud vs. radio quiet
- jets & radio lobes
- blazar phenomenology

Phenomenology

The model should also be able to explain:

- nature of continuum emission
- nature of line emission
- broad lines vs. narrow lines
- radio loud vs. radio quiet
- jets & radio lobes
- blazar phenomenology

Phenomenology

The model should also be able to explain:

- nature of continuum emission
- nature of line emission
- broad lines vs. narrow lines
- radio loud vs. radio quiet
- jets & radio lobes
- blazar phenomenology

Phenomenology

The model should also be able to explain:

- nature of continuum emission
- nature of line emission
- broad lines vs. narrow lines
- radio loud vs. radio quiet
- jets & radio lobes
- blazar phenomenology

The SMBH model

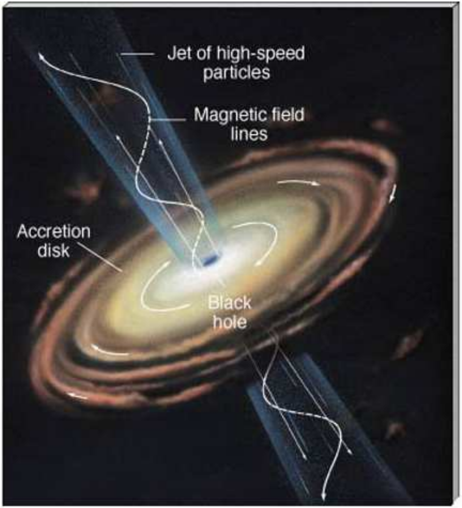

The SMBH model

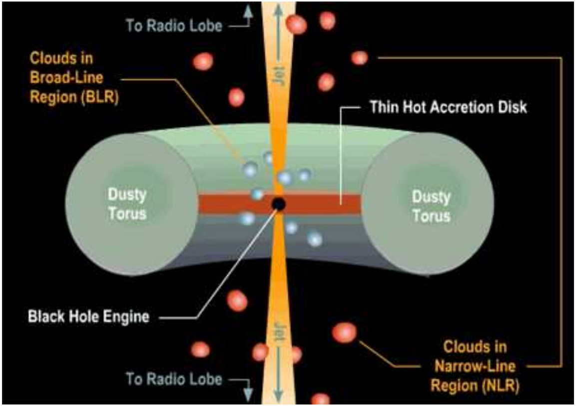

(Brooks/Cole Thomson Learning)

The SMBH model

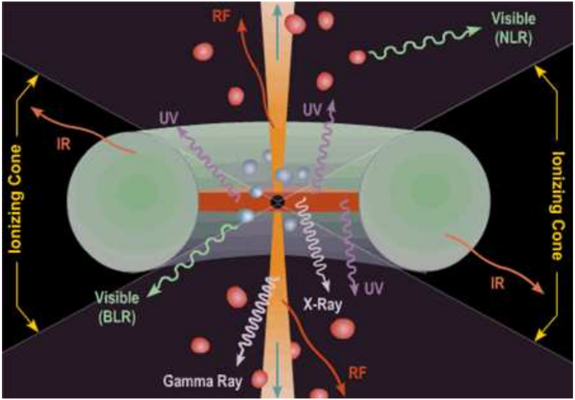

(Brooks/Cole Thomson Learning)

Emission properties

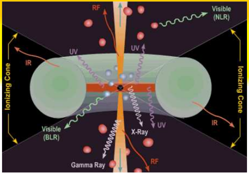

component	emission mechanism	spectral range
accretion disk	thermal ($T \lesssim 10^5$ K)	optical $\rightarrow$ soft X-rays
dusty torus	reprocessed AD emission	sub-mm $\rightarrow$ IR
BLR – NLR	recombination in photo-ionized gas	optical (emission line spectrum)
jet	synchrotron	radio
	non-thermal (inverse Compton)	up to γ-rays

Emission properties

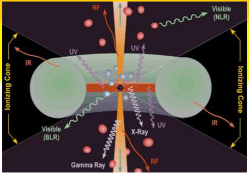

component	emission mechanism	spectral range
accretion disk	thermal ($T \lesssim 10^5$ K)	optical $\rightarrow$ soft X-rays
dusty torus	reprocessed AD emission	sub-mm $\rightarrow$ IR
BLR – NLR	recombination in photo-ionized gas	optical (emission line spectrum)
jet	synchrotron	radio
	non-thermal (inverse Compton)	up to γ-rays

Emission properties

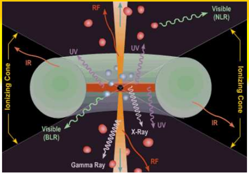

component	emission mechanism	spectral range
accretion disk	thermal ($T \lesssim 10^5$ K)	optical $\rightarrow$ soft X-rays
dusty torus	reprocessed AD emission	sub-mm $\rightarrow$ IR
BLR – NLR	recombination in photo-ionized gas	optical (emission line spectrum)
jet	synchrotron	radio
	non-thermal (inverse Compton)	up to γ-rays

Emission properties

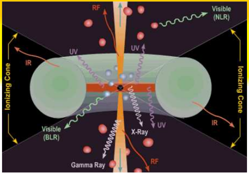

component	emission mechanism	spectral range
accretion disk	thermal ($T \lesssim 10^5$ K)	optical $\rightarrow$ soft X-rays
dusty torus	reprocessed AD emission	sub-mm $\rightarrow$ IR
BLR – NLR	recombination in photo-ionized gas	optical (emission line spectrum)
jet	synchrotron	radio
	non-thermal (inverse Compton)	up to γ-rays

Emission properties

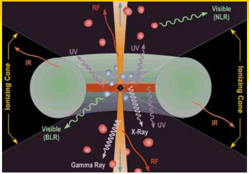

component	emission mechanism	spectral range
accretion disk	thermal ($T \lesssim 10^5$ K)	optical $\rightarrow$ soft X-rays
dusty torus	reprocessed AD emission	sub-mm $\rightarrow$ IR
BLR – NLR	recombination in photo-ionized gas	optical (emission line spectrum)
jet	synchrotron	radio
	non-thermal (inverse Compton)	up to γ-rays

Emission properties

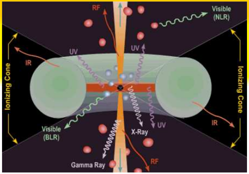

component	emission mechanism	spectral range
accretion disk	thermal ($T \lesssim 10^5$ K)	optical $\rightarrow$ soft X-rays
dusty torus	reprocessed AD emission	sub-mm $\rightarrow$ IR
BLR – NLR	recombination in photo-ionized gas	optical (emission line spectrum)
jet	synchrotron	radio
	non-thermal (inverse Compton)	up to γ-rays

Continuum emission

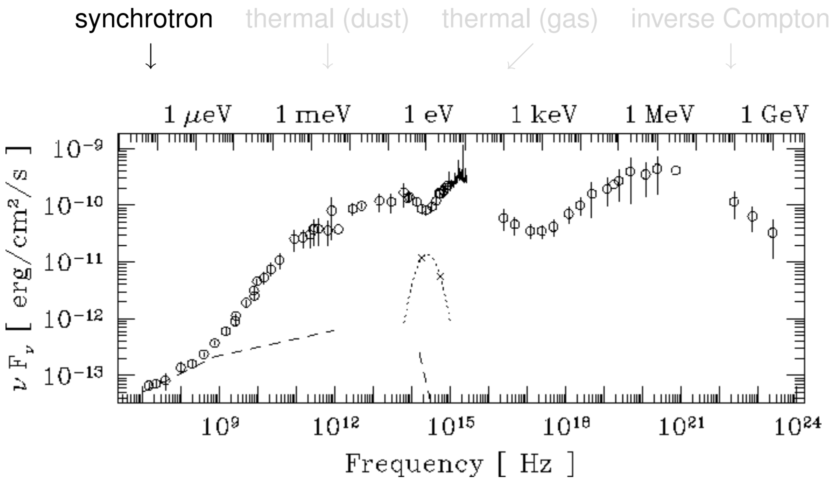

Continuum emission

synchrotron thermal (dust) thermal (gas) inverse Compton

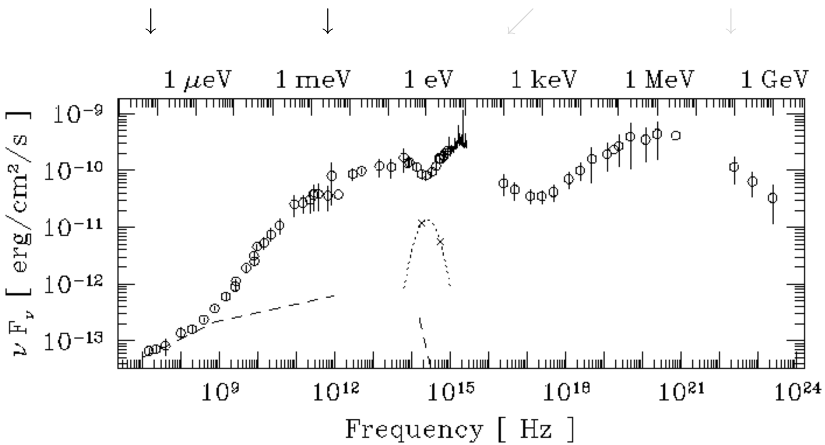

Continuum emission

synchrotron ↓ thermal (dust) ↓ thermal (gas) ↙ inverse Compton ↓

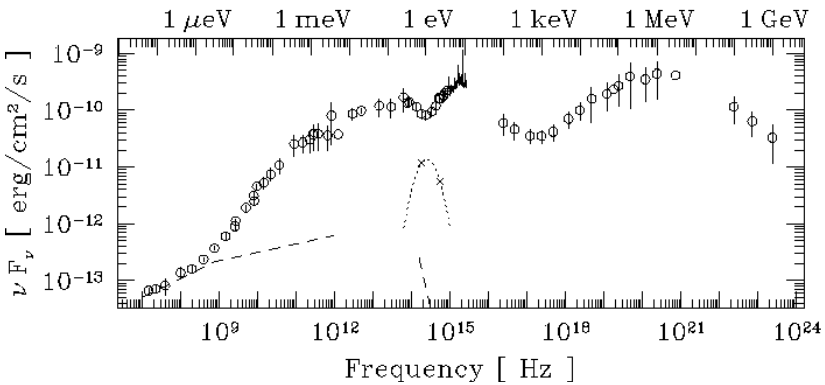

Continuum emission

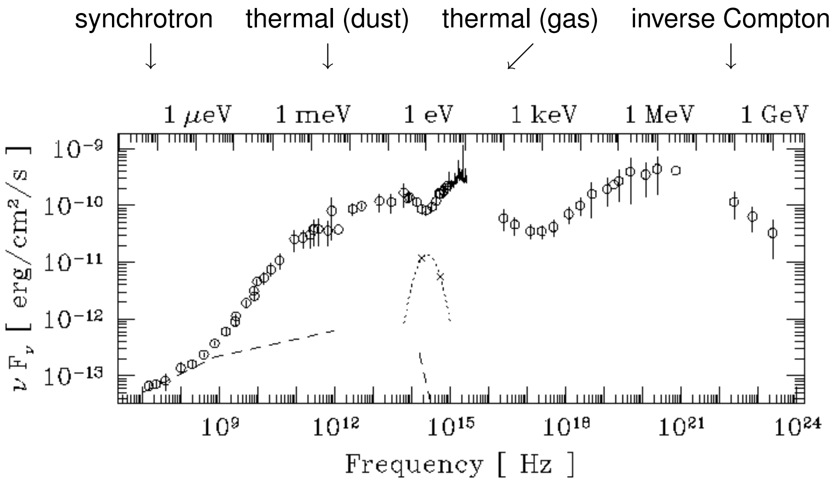

Continuum emission

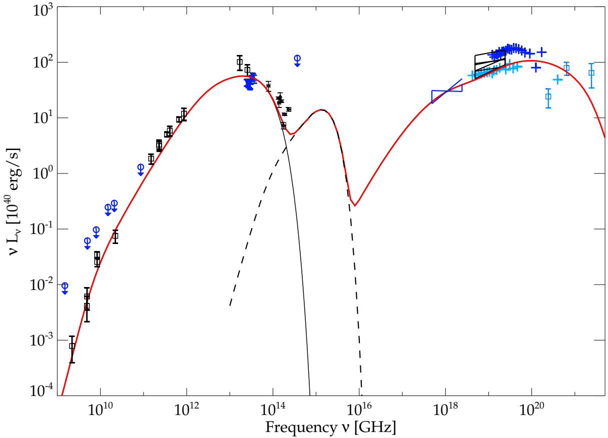

(Prieto et al. 2007)

Cen A: non-thermal contribution in the mid – far IR

Unification

Broad lines vs. narrow lines

NGC 1068
(Antonucci & Miller 1985):

- “normal” light → Sy 2
- polarized light → Sy 1 features

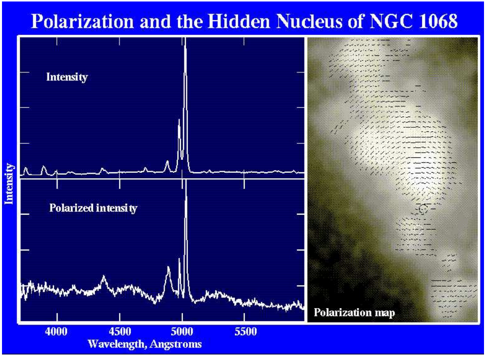

BLR light scattered by electrons into the line of sight

Unification

Broad lines vs. narrow lines

NGC 1068
(Antonucci & Miller 1985):

- “normal” light → Sy 2
- polarized light → Sy 1 features

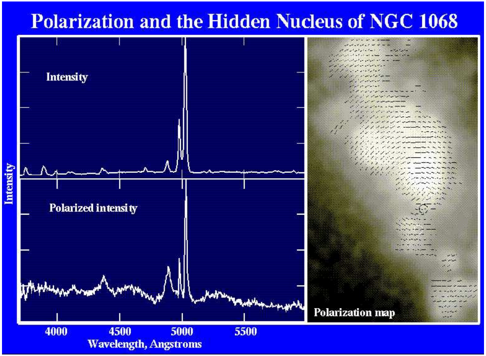

BLR light scattered by electrons into the line of sight

Unification

Broad lines vs. narrow lines

NGC 1068
(Antonucci & Miller 1985):

- “normal” light → Sy 2
- polarized light → Sy 1 features

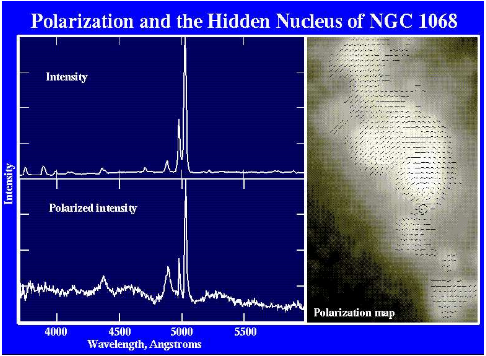

BLR light scattered by electrons into the line of sight

Unification

- obscuration
- beaming

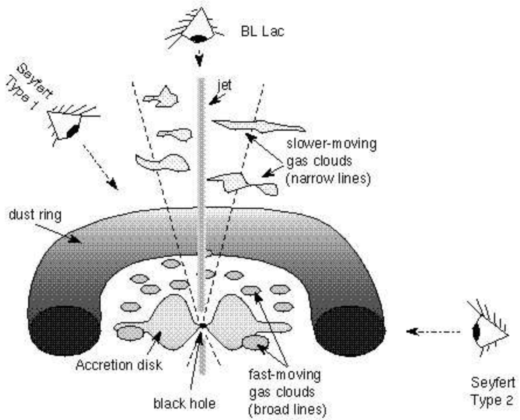

Unification

- obscuration
- beaming

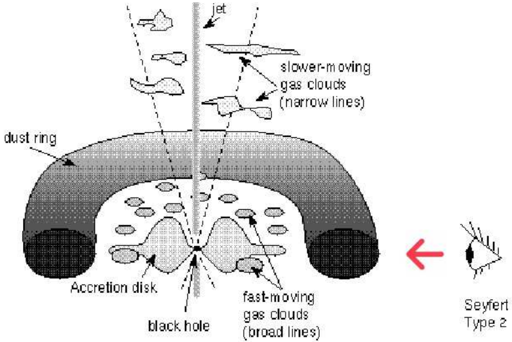

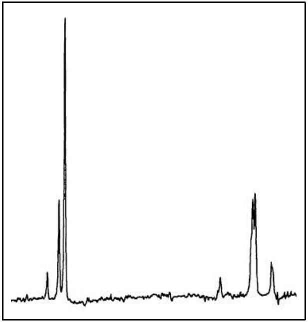

Sy 2 or NLRG
(or “obscured” QSO)

Unification

- obscuration
- beaming

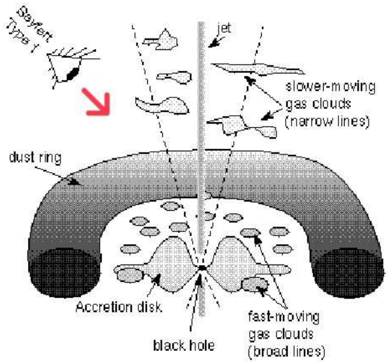

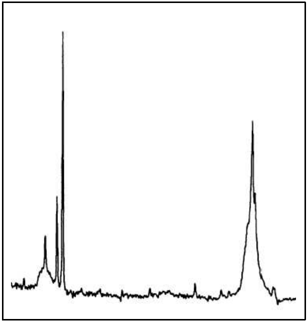

Sy 1 or BLRG
(or “normal” QSO)

Unification

- obscuration
- beaming

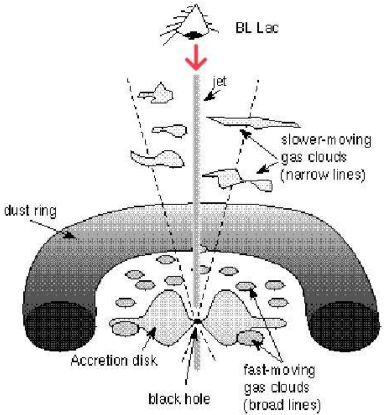

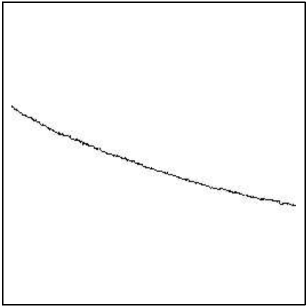

blazar

Blazars

The wildest of all beasts

BL Lacs + FSRQs = blazars

- Strong emission from radio to γ-rays
- Fast, high-amplitude flux variability
- High and variable polarization
- Superluminal motions (radio jet)

Blazars

Relativistic beaming

Plasma with bulk motion $\beta = \frac{v}{c} \lesssim 1$ and angle $\theta \gtrsim 0^\circ$

$\rightarrow$ emission is beamed in the observer's direction

Lorentz factor: $\gamma = (1 - \beta^2)^{-\frac{1}{2}}$

Doppler factor: $\delta = [\gamma(1 - \beta \cos\theta)]^{-1}$

	rest frame	observer's frame
time interval	t	$\delta^{-1} t$
frequency	ν	$\delta\, \nu$
intensity	$I_\nu(\nu)$	$\delta^3 I_\nu(\nu)$
flux density	$F_\nu(\nu)$	$\delta^{(3+\alpha)} F_\nu(\nu)$
broad-band flux	F	$\delta^4 F$

Blazars

Relativistic beaming

Plasma with bulk motion $\beta = \frac{v}{c} \lesssim 1$ and angle $\theta \gtrsim 0^\circ$

$\rightarrow$ emission is beamed in the observer's direction

Lorentz factor: $\gamma = (1 - \beta^2)^{-\frac{1}{2}}$

Doppler factor: $\delta = [\gamma(1 - \beta \cos\theta)]^{-1}$

	rest frame	observer's frame
time interval	t	$\delta^{-1} t$
frequency	ν	$\delta\, \nu$
intensity	$I_\nu(\nu)$	$\delta^3 I_\nu(\nu)$
flux density	$F_\nu(\nu)$	$\delta^{(3+\alpha)} F_\nu(\nu)$
broad-band flux	F	$\delta^4 F$

Blazars
Relativistic beaming

Plasma with bulk motion $\beta = \frac{v}{c} \lesssim 1$ and angle $\theta \gtrsim 0^\circ$
$\longrightarrow$ emission is beamed in the observer's direction

Lorentz factor: $\gamma = (1 - \beta^2)^{-\frac{1}{2}}$
Doppler factor: $\delta = [\gamma(1 - \beta \cos\theta)]^{-1}$

	rest frame	observer's frame
time interval	t	$\delta^{-1} t$
frequency	ν	$\delta\,\nu$
intensity	$I_\nu(\nu)$	$\delta^3 I_\nu(\nu)$
flux density	$F_\nu(\nu)$	$\delta^{(3+\alpha)} F_\nu(\nu)$
broad-band flux	F	$\delta^4 F$

Blazars
Relativistic beaming

Plasma with bulk motion $\beta = \frac{v}{c} \lesssim 1$ and angle $\theta \gtrsim 0^\circ$
$\longrightarrow$ emission is beamed in the observer's direction

Lorentz factor: $\gamma = (1 - \beta^2)^{-\frac{1}{2}}$

Doppler factor: $\delta = [\gamma(1 - \beta \cos\theta)]^{-1}$

	rest frame	observer's frame
time interval	t	$\delta^{-1} t$
frequency	ν	$\delta\, \nu$
intensity	$I_\nu(\nu)$	$\delta^3 I_\nu(\nu)$
flux density	$F_\nu(\nu)$	$\delta^{(3+\alpha)} F_\nu(\nu)$
broad-band flux	F	$\delta^4 F$

Blazars

Relativistic beaming

Plasma with bulk motion $\beta = \frac{v}{c} = 0.99$ and angle $\theta = 5^\circ$

Lorentz factor: $\gamma = (1 - \beta^2)^{-\frac{1}{2}} = 7.$

Doppler factor: $\delta = [\gamma(1 - \beta \cos\theta)]^{-1} = 10.$

	rest frame	observer's frame	example
time interval	t	$\delta^{-1} t$	$0.1\, t$
frequency	ν	$\delta\, \nu$	$10\, \nu$
intensity	$I_\nu(\nu)$	$\delta^3 I_\nu(\nu)$	$10^3 I_\nu(\nu)$
flux density	$F_\nu(\nu)$	$\delta^{(3+\alpha)} F_\nu(\nu)$	$10^{(3+\alpha)} F_\nu(\nu)$
broad-band flux	F	$\delta^4 F$	$10^4 F$

Blazars

Spectral energy distribution

synchrotron ↓ inverse Compton ↓

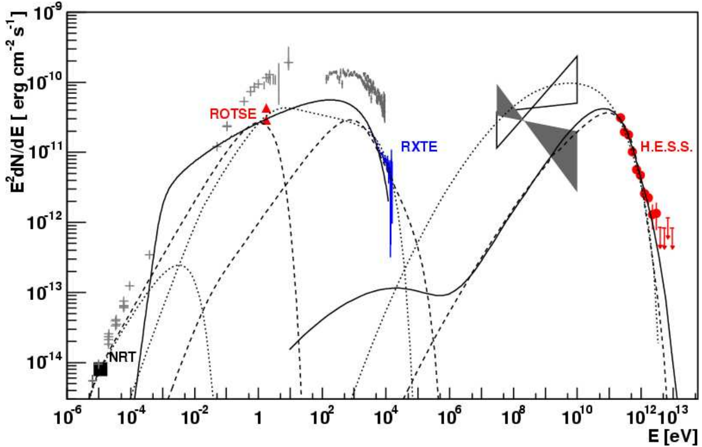

(Aharonian et al. 2005, A&A, 442, 895)

Blazars
Spectral energy distribution

synchrotron
↓
inverse Compton
↓

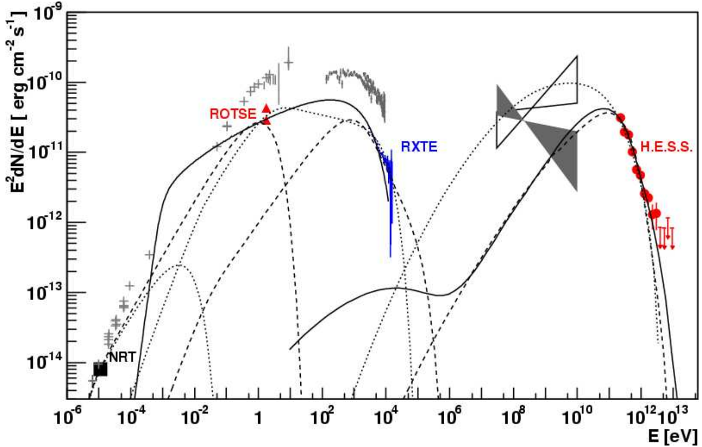

(Aharonian et al. 2005, A&A, 442, 895)

Alternative models

Terlevich et al. (1992):

AGN phenomenology explained by starburts

Previous dichotomy “monster” vs. starburst
now replaced by realization that
each phenomenon has its own significance

Alternative models

Terlevich et al. (1992):

AGN phenomenology explained by starburts

Previous dichotomy "monster" vs. starburst
now replaced by realization that
each phenomenon has its own significance

The radio-loud radio-quiet dichotomy

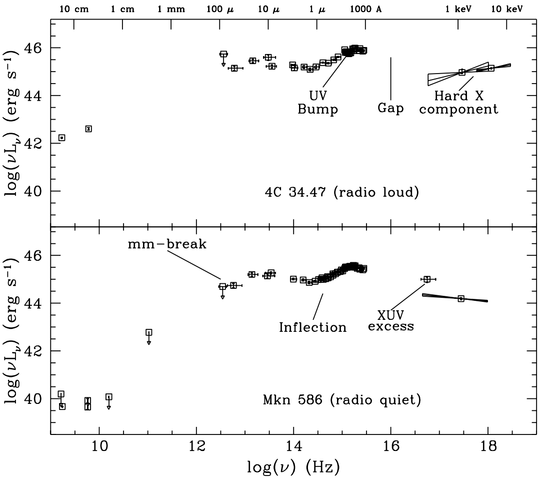

The radio-loud radio-quiet dichotomy

The SEDs of RL and RQ quasars do not differ at higher frequencies

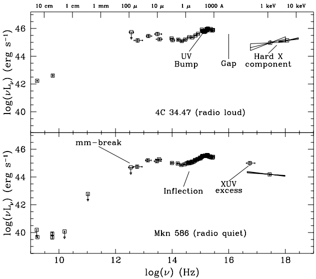

The existence or not of a radio jet is basically independent from accretion

The radio-loud radio-quiet dichotomy

The SEDs of RL and RQ quasars do not differ at higher frequencies

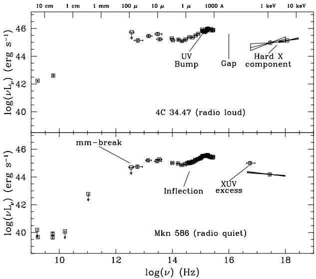

The existence or not of a radio jet
is basically independent from accretion

The radio-loud radio-quiet dichotomy

RL AGN: never in S galaxies
RQ AGN: rarely in E galaxies

(e.g., Wilson & Colbert 1995)

Galaxy mergers $\longrightarrow$
E galaxies with spinning SMBH

$\Downarrow$

Radio jet powered by SMBH spin

The radio-loud radio-quiet dichotomy

RL AGN: never in S galaxies

RQ AGN: rarely in E galaxies

(e.g., Wilson & Colbert 1995)

Galaxy mergers $\rightarrow$
E galaxies with spinning SMBH

$\Downarrow$

Radio jet powered by SMBH spin

The radio-loud radio-quiet dichotomy

RL AGN: never in S galaxies

RQ AGN: rarely in E galaxies

(e.g., Wilson & Colbert 1995)

Galaxy mergers →
E galaxies with spinning SMBH

⇓

Radio jet powered by SMBH spin

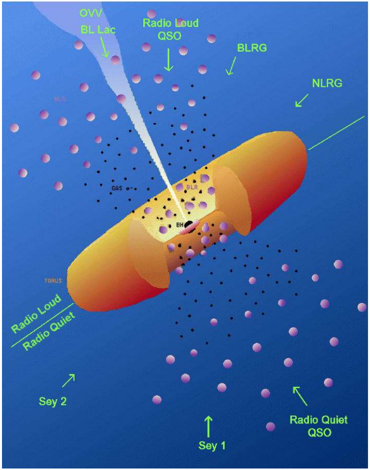

Spatial scale

Approximate sizes for components of an AGN
$\mathcal{M}_{\rm BH} = 10^8 \mathcal{M}_\odot$, $d = 1$ Gpc

Region	Size		
	[LTT]	[AU] – [pc]	[arcsec]
R_S	15 min	2 AU	2×10^{-9}
AD	1 h $\sim$ 1 d	7 $\sim$ 200 AU	$7 \times 10^{-9} \sim 2 \times 10^{-7}$
BLR	8 $\sim$ 80 d	$10^3 \sim 10^4$ AU	$10^{-6} \sim 10^{-5}$
$R_{\rm DT}$ (inn.)	$\sim$ 40 d	$\sim 5 \times 10^3$ AU	5×10^{-6}
NLR	1 $\sim$ 100 yr	0.3 $\sim$ 30 pc	$5 \times 10^{-5} \sim 5 \times 10^{-3}$
radio jets	$\lesssim 10^6$ yr	$\lesssim$ 300 kpc	$\lesssim 60$

Spatial scale

Approximate sizes for components of an AGN
$\mathcal{M}_{\rm BH} = 10^8 \mathcal{M}_\odot$, $d = 1$ Gpc

Region	**Size** [LTT]	[AU] – [pc]	[arcsec]
R_S	15 min	2 AU	2×10^{-9}
AD	1 h $\sim$ 1 d	7 $\sim$ 200 AU	$7 \times 10^{-9} \sim 2 \times 10^{-7}$
BLR	8 $\sim$ 80 d	$10^3 \sim 10^4$ AU	$10^{-6} \sim 10^{-5}$
$R_{\rm DT}$ (inn.)	$\sim$ 40 d	$\sim 5 \times 10^3$ AU	5×10^{-6}
NLR	1 $\sim$ 100 yr	0.3 $\sim$ 30 pc	$5 \times 10^{-5} \sim 5 \times 10^{-3}$
radio jets	$\lesssim 10^6$ yr	$\lesssim$ 300 kpc	$\lesssim 60$

Spatial scale

Approximate sizes for components of an AGN
$\mathcal{M}_{BH} = 10^8 \mathcal{M}_\odot$, $d = 1$ Gpc

Region	Size [LTT]	[AU] – [pc]	[arcsec]
R_S	15 min	2 AU	2×10^{-9}
AD	1 h $\sim$ 1 d	7 $\sim$ 200 AU	$7 \times 10^{-9} \sim 2 \times 10^{-7}$
BLR	8 $\sim$ 80 d	$10^3 \sim 10^4$ AU	$10^{-6} \sim 10^{-5}$
R_{DT} (inn.)	$\sim$ 40 d	$\sim 5 \times 10^3$ AU	5×10^{-6}
NLR	1 $\sim$ 100 yr	0.3 $\sim$ 30 pc	$5 \times 10^{-5} \sim 5 \times 10^{-3}$
radio jets	$\lesssim 10^6$ yr	$\lesssim$ 300 kpc	$\lesssim 60$

Active Galactic Nuclei

Radio interferometry

Evidence for a gas disc

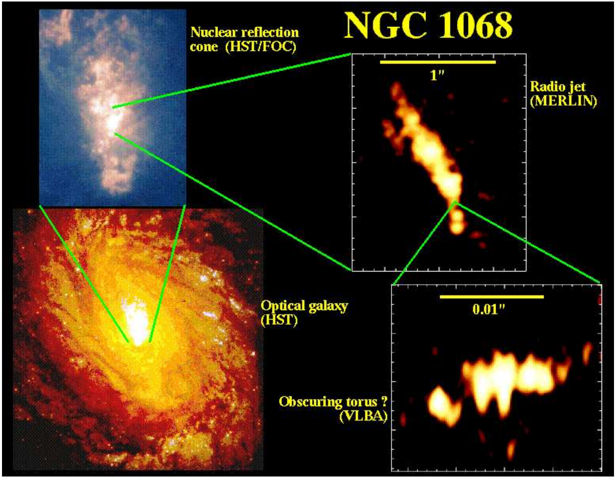

Gallimore et al. (1997)

$$d = 15.1\,\text{Mpc}$$
$$\Downarrow$$
$$1'' \equiv 75\,\text{pc}$$
$$0\farcs01 \equiv 0.75\,\text{pc}$$

Radio interferometry

Gas disc rotation

Syfert galaxy NGC 4258:
22 GHz (μ-wave) maser emission

annulus:
$D_{\rm inn} = 0.13\,{\rm pc}$ — $D_{\rm out} = 0.26\,{\rm pc}$
$\Rightarrow \quad 3.6 \times 10^7\,\mathcal{M}_\odot$
within $R \lesssim 0.012\,{\rm pc}$ ($\equiv$ 2500 AU)

(Miyoshi et al. 1995)

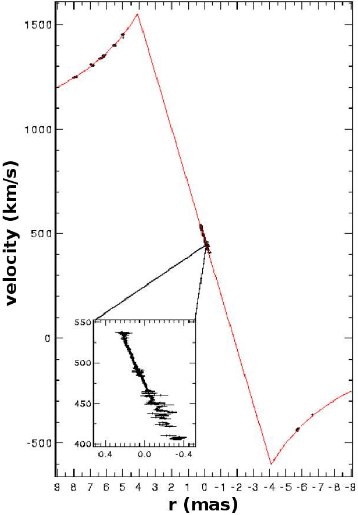

Optical (HST)

Gas disc rotation

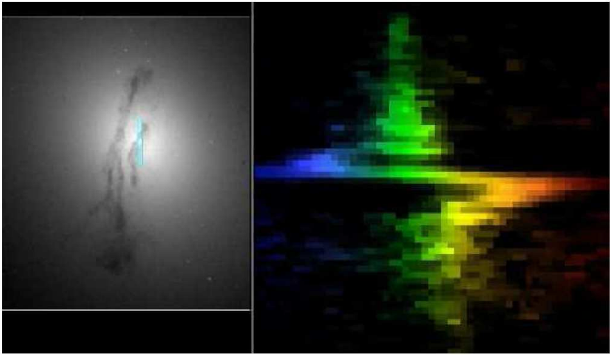

(Bower et al. 1997, 1998)

M 84 ($d = 17$ Mpc): central $3''$ ($\equiv 240$ pc) Hα spectrum
disc: $D \simeq 80$ pc; $\Delta v = 1445$ km s^{-1} $\Rightarrow \mathcal{M}_{\rm BH} \simeq 2 \times 10^9 \mathcal{M}_\odot$

Optical (HST)
Binary BH signatures

Balmaverde & Capetti (2006):
core galaxies invariably host
a radio-loud nucleus

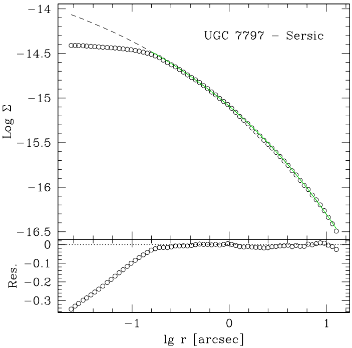

X-rays (Chandra)
Binary AGN

Bianchi et al. (2008): Binary AGN in Mrk 463

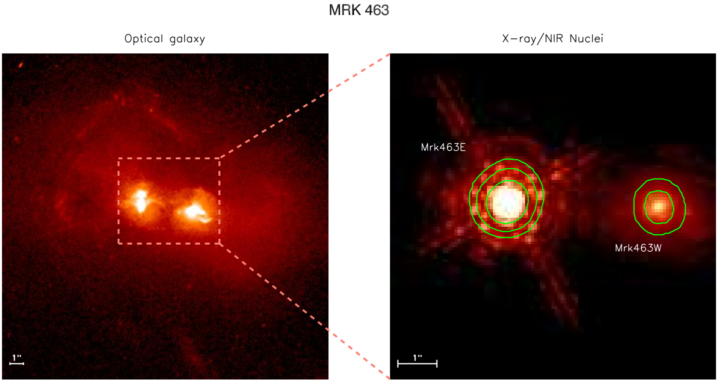

Reverberation mapping

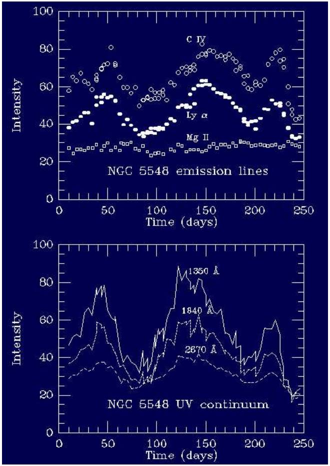

Reverberation mapping

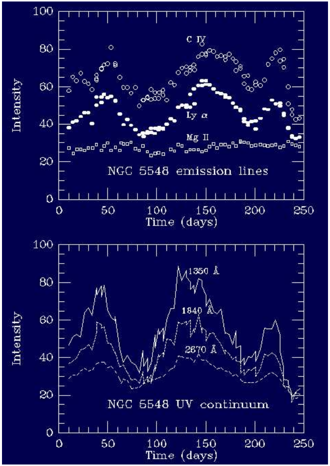

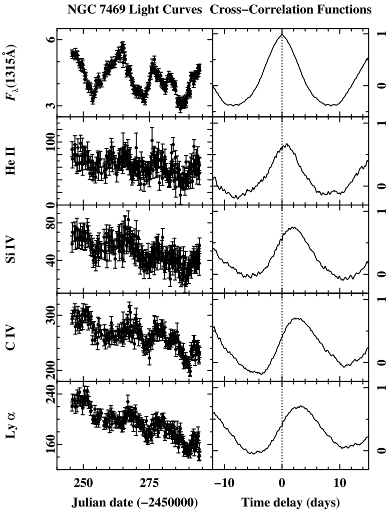

(Netzer & Peterson 1997)

Reverberation mapping

Line variability delayed $\tau = \frac{r}{c}(1 + \cos\theta)$ with respect to UV flux variability

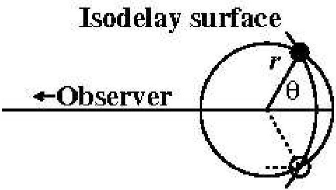

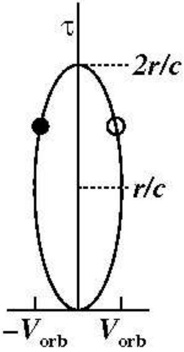

$R_{\rm BLR} \propto L^{\frac{1}{2}}$

Measure of $\mathcal{M}_{\rm BH}$

Reverberation mapping

Line variability delayed $\tau = \frac{r}{c}(1 + \cos\theta)$
with respect to UV flux variability

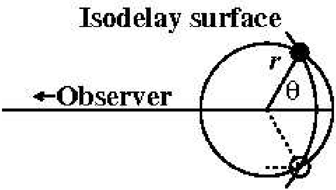

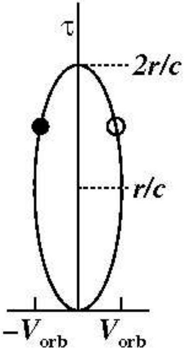

$R_{\mathrm{BLR}} \propto L^{\frac{1}{2}}$
Measure of $\mathcal{M}_{\mathrm{BH}}$

Disk-jet interaction

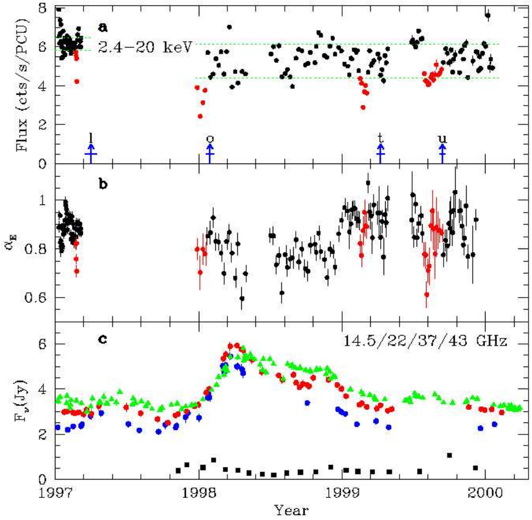

3C 120
(BLRG)

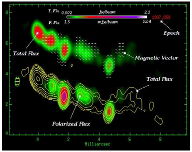

RXTE + VLBI
(Marscher et al. 2002)

Polarimetric microvariability

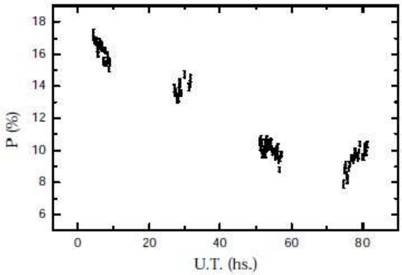

blazar 3C 279

$\Delta\theta \sim 2^\circ \Rightarrow \Delta P \simeq 10\,\%$

(Andruchow et al. 2003)

Polarimetric microvariability

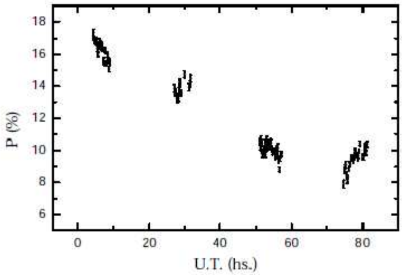

blazar 3C 279

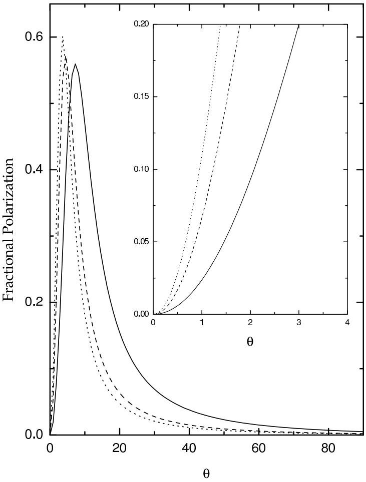

$\Delta\theta \sim 2^{\circ} \Rightarrow \Delta P \simeq 10\,\%$

(Andruchow et al. 2003)

Polarimetric microvariability

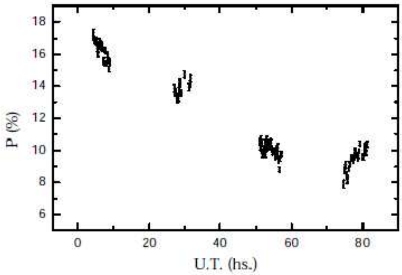

blazar 3C 279

$$\Delta\theta \sim 2^\circ \Rightarrow \Delta P \simeq 10\,\%$$

(Andruchow et al. 2003)

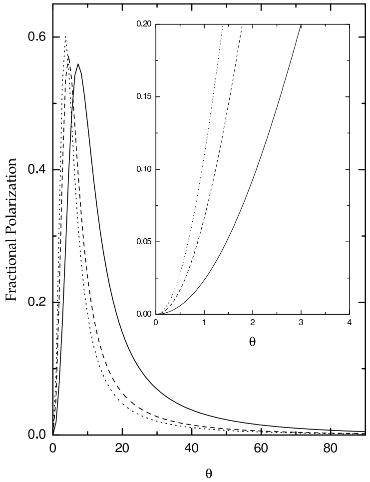

Extremely violent microvariability?

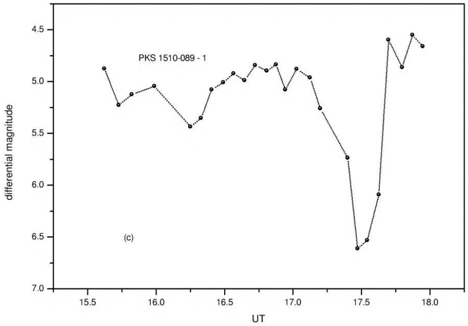

PKS 1510-089

$\Delta R \simeq 2\,\mathrm{mag}$ in $\sim 40\,\mathrm{min}$ (Dai et al. 2001)

$\Delta R \simeq 1.3\,\mathrm{mag}$ in $\sim 90\,\mathrm{min}$ (Xie et al. 2004)

Extremely violent microvariability?
Not so

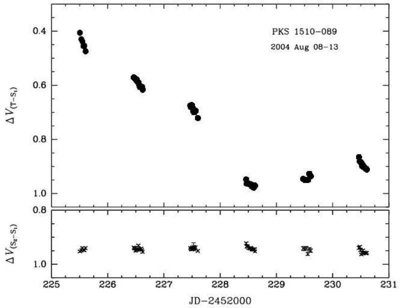

PKS 1510-089

(Cellone, Romero, & Araudo 2007)

$\Delta V \simeq 0.6$ mag in ~ 4 days

$\Delta V \lesssim 0.1$ mag in ~ 1 hr

Extremely violent microvariability?
Not so

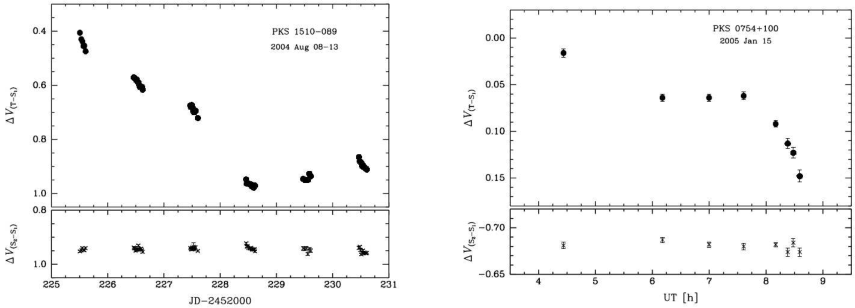

PKS 1510-089

(Cellone, Romero, & Araudo 2007)
$\Delta V \simeq 0.6$ mag in $\sim$ 4 days
$\Delta V \lesssim 0.1$ mag in $\sim$ 1 hr

Extremely violent microvariability?

Not so

Significance of the variability: $\frac{\sigma_T}{\sigma_2}$

Howell et al. (1988):
Statistical error analysis in CCD time-resolved photometry with applications to variable stars and quasars

$$\Gamma^2 = \left(\frac{N_2}{N_T}\right)^2 \left[\frac{N_1^2(N_T + P) + N_T^2(N_1 + P)}{N_2^2(N_T + P) + N_T^2(N_2 + P)}\right]$$

$$\frac{\sigma_T}{\Gamma\ \sigma_2}$$

Extremely violent microvariability?

Not so

Significance of the variability: $\frac{\sigma_T}{\sigma_2}$

Howell et al. (1988):
Statistical error analysis in CCD time-resolved photometry with applications to variable stars and quasars

$$\Gamma^2 = \left(\frac{N_2}{N_T}\right)^2 \left[\frac{N_1^2(N_T + P) + N_T^2(N_1 + P)}{N_2^2(N_T + P) + N_T^2(N_2 + P)}\right]$$

$$\frac{\sigma_T}{\Gamma\ \sigma_2}$$

Extremely violent microvariability?

Not so

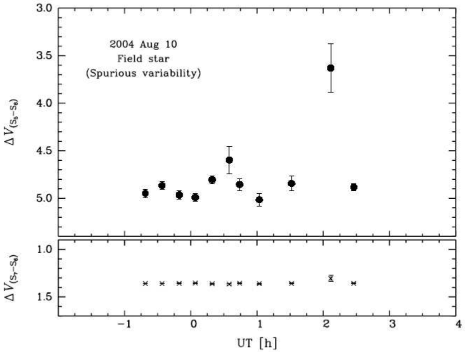

test using an incorrect photometric technique

Field star

$\Delta V \simeq 1.2^{\text{mag}}$ in ~ 35 min

$$\frac{\sigma_T}{\sigma_2} = 24.0$$

$$\frac{\sigma_T}{\Gamma\, \sigma_2} = 1.0$$

$\longrightarrow$ spurious variability!

Extremely violent microvariability?
Not so

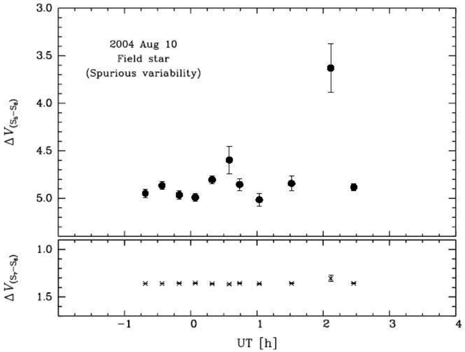

test using an incorrect photometric technique

Field star

$\Delta V \simeq 1.2^{mag}$ in ~ 35 min

$$\frac{\sigma_T}{\sigma_2} = 24.0$$

$$\frac{\sigma_T}{\Gamma\,\sigma_2} = 1.0$$

$\longrightarrow$ spurious variability!

BH mass

The BH mass can be measured by:

- optical emission line widths (BLR)
- gas dynamics (radio – optical)
- reverberation mapping
- accretion disk spectrum
- X-ray variability

BH mass

A $2.6 \times 10^6\,\mathcal{M}_\odot$ BH
at the centre of the Milky Way

(Schödel et al. 2002)

The BH mass vs. bulge mass relation

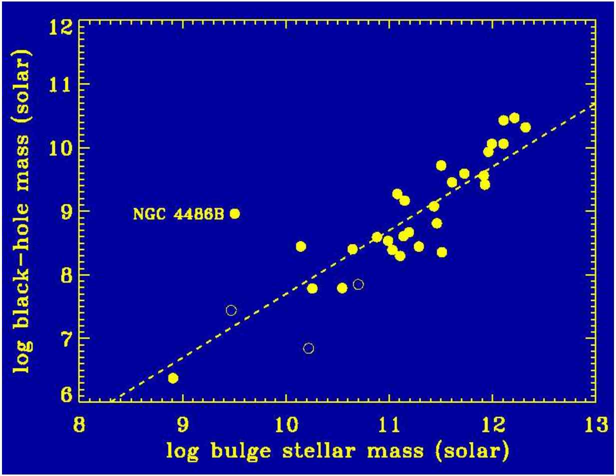

The BH mass vs. bulge mass relation

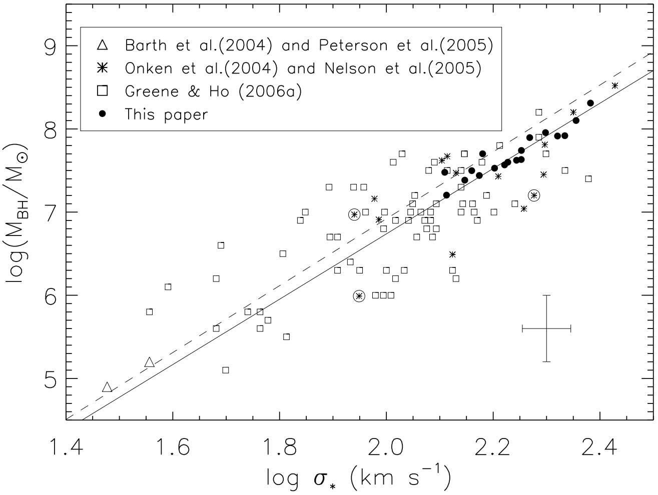

(Shen et al. 2007)

The AGN stage

BH lie at the centres of massive spheroids
(E galaxies and bulges)

Nuclear activity needs gas supply

- interactions / mergers
- bars
- inner disks

. . . etc.